JOURNAL OF MATERIALS SCIENCE 28 (1993) 5725–5730

Compressibility measurements of β- and β″-alumina

H. ARASHI, H. NAITO, A. KAIMAI
Research Institute for Scientific Measurements, Tohoku University, 2-1-1 Katahira, Sendai 980, Japan

The compressibilities of the *a*- and *c*-axes for sodium β- and β″-aluminas were determined up to 10 GPa from the pressure dependence of powder X-ray diffraction measured at room temperature using synchrotron radiation as an X-ray source. Powders of sodium β- and β″-aluminas which were prepared from grinding synthesized single crystals were used as the specimens for X-ray diffraction. The compressibilities of β- and β″-aluminas are $1.5 \pm 0.2 \times 10^{-12}$ and $1.7 \pm 0.2 \times 10^{-12}$ Pa^{-1} for the *a*-axis and $2.9 \pm 0.2 \times 10^{-12}$ and $1.6 \pm 0.2 \times 10^{-12}$ Pa^{-1} for the *c*-axis, respectively. For the *c*-axis, the compressibility of β-alumina is larger than that of β″-alumina. This experimental fact is explained by the different stacking of oxygen layers and the different content in sodium ion between β- and β″-aluminas.

1. Introduction

The β- and β″-aluminas have a very high ionic conductivity in the medium temperature range from room temperature to 500 °C. Therefore, the β- and β″-aluminas are the most important solid electrolytes, not only because of their practical usefulness such as in Na/S batteries, but also because of their typical two-dimensional ionic conducting properties which provide the theoretical basis for the clarification of the ionic conduction mechanism in solids [1–4].

The pressure effect which changes the inter-atomic distance has a large influence on ionic conduction in solids. The pressure dependence of ionic conductivity for β-alumina has been reported by several workers [5, 6]. They could infer the ionic conduction mechanism from the pressure dependence of ionic conductivity. In these experiments, precise measurements of the compressibilities of the *a*- and *c*-axes for these aluminas are indispensable to deduce the proper conclusions. Until now, little investigation of the compressibility of β-alumina has been reported [7].

Recently, molecular dynamics using a computer simulation was applied to theoretically investigate the ionic conduction mechanism in fast ion conductors [8, 9]. In that investigation the potential parameters among the constituent ions in the crystal were the dominating factors to determine the ionic motion concerned with ionic conduction. The compressibility data of the crystal play an important role in deducing these potential parameters.

From this point of view, the compressibilities of β- and β″-aluminas were measured from the pressure dependence of the lattice constants of the *a*- and *c*-axes determined by X-ray diffraction at room temperature using synchrotron radiation as an X-ray source.

2. Experimental procedure

Compressibilities of β- and β″-aluminas were determined from the pressure dependence of lattice constants measured by powder X-ray diffraction at high pressures. An *in situ* X-ray diffraction study was performed using the "MAX80" multi-anvil high-pressure apparatus installed in the Photon Factory at the Synchrotron Radiation Facility of the National Laboratory for High Energy Physics (Tsukuba, Japan). Synchrotron radiation with operating conditions of 6.4 GeV and 30 mA was used as a white X-ray source. The details of this system are described elsewhere [10, 11].

The single crystal of sodium β-alumina was provided by Toshiba Co. Ltd. The single crystal of sodium β″-alumina was grown at 1700 °C from a melt of Na_2O, MgO and Al_2O_3 using a platinum crucible. These synthesized crystals were ground with an alumina mortar and passed through a 300 mesh sieve under a dried nitrogen atmosphere.

The sample assembly used for the present study is presented in Fig. 1. Two 6 × 6 × 3 mm blocks of 4:1 boron–epoxy resin mixture were used as a pressure-transmitting medium. A cylindrical hole (2 mm in diameter) was drilled through the center of these blocks. In order to maintain the hydrostatic property of pressure, β- and β″-alumina powders were loaded into a teflon vessel filled with a pressure-transmitting liquid, a 4:1 mixture of methanol and ethanol. This teflon vessel was placed into the central hole of the upper block. The central hole of the lower block was filled with NaCl powder, which was used as a pressure marker. Pressure was determined from the volume change of NaCl using Decker's equation of state [12]. With this pressure cell and sample assembly the

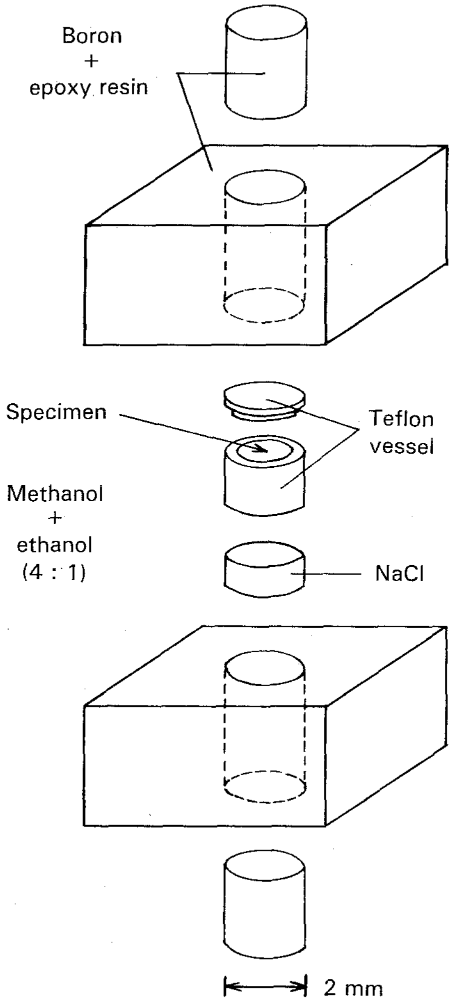

Figure 1 Sample assembly of the "MAX80" high-pressure X-ray diffraction measuring system.

maximum pressure of 10 GPa was stably obtained. X-ray intensity diffracted at 10° in 2θ was measured by an energy dispersive method using a pure germanium detector. The energy resolution of this detector was about 30 eV in the energy region 20–50 keV. The absolute energy value was calibrated against the fluorescence of Fe, Cu, Mo, Ag and Sn. Diffracted X-rays were collected in a multi-channel pulse-height analyser for 1000–3000 s and the acquired data were transferred to a computer system to carry out curve fitting of the measured diffraction peak, in order to accurately determine the peak position.

3. Results and discussions

The structures of β- and β″-alumina are well established. β-alumina takes hexagonal symmetry and its space group is assigned to $P6_3/mmc$. β″-alumina takes rhombohedral symmetry and its space group is assigned to $R\bar{3}$. The X-ray diffraction patterns of sodium β- and β″-alumina measured using the "MAX80" under ambient conditions are presented in Fig. 2. X-ray diffraction studies of these crystals have been reported by many workers [13–15]. The measured patterns were indexed by referring to these reports. This indexing agreed well with that of the most recent JCPDS files (32-1033, 31-1262 for β- and β″-alumina, respectively). The relative intensity of the diffraction peaks is different from the JCPDS data. This difference can be explained by the layered structure of these crystals and the highly collimated X-ray source from the synchrotron. The orientation of crystals was not fully randomized because of these effects. Therefore, the relative intensity changes with deformation of the sample assembly induced by pressure loading, as shown in Fig. 3.

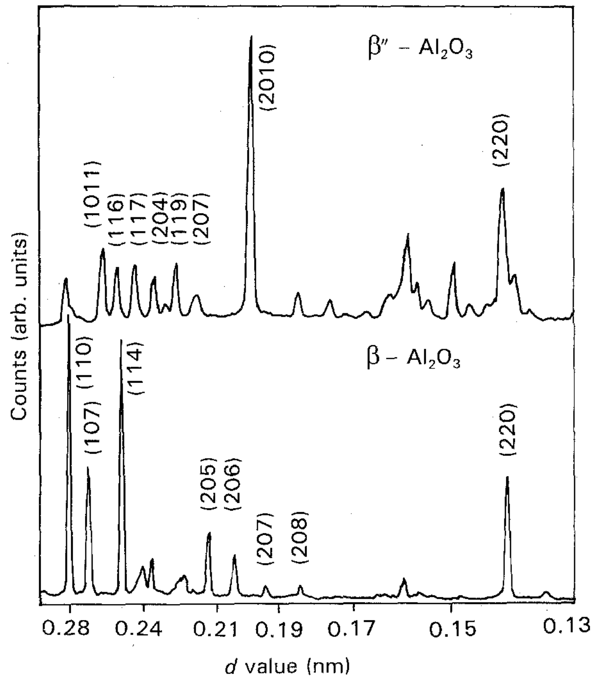

Figure 2 X-ray diffraction patterns of β- and β″-aluminas measured under ambient conditions using the "MAX80" system.

The measured *d* values were precisely determined from the curve fitting between the measured line shape and theoretical Lorentzian line shape. The lattice constants of the *a*- and *c*-axes were determined by minimizing the sum of square values of difference between calculated and measured *d* values for eight diffraction peaks, indexed as shown in Fig. 2. This method was applied to the JCPDS files and the same values for *a*- and *c*-axes were obtained as shown in Table I. Therefore, it is considered that this method is appropriate for determination of the lattice constants in our experiments. The *d* values of sodium β- and β″-alumina calculated by using the lattice constants of the *a*- and *c*-axes determined with this method are also compared with the measured values under ambient conditions in Table I. As the agreement between calculated and observed value was very good, this method can be used to analyse the X-ray diffraction patterns measured at high pressures and to determine the pressure dependence of the lattice constants of the *a*- and *c*-axes. The accuracy of the determination of lattice constants is fixed by the energy resolution of the employed Ge detector. In our experimental system the energy resolution of the detector is 30 eV. This value is assigned to an accuracy of 0.005 Å and 0.05 Å for the *a*- and *c*-axes, respectively. The lattice constants of sodium β″-alumina measured by using the "MAX80" are different from that of the JCPDS files. This difference is assigned to the difference in sodium contents [16]. The pressure dependence of the X-ray

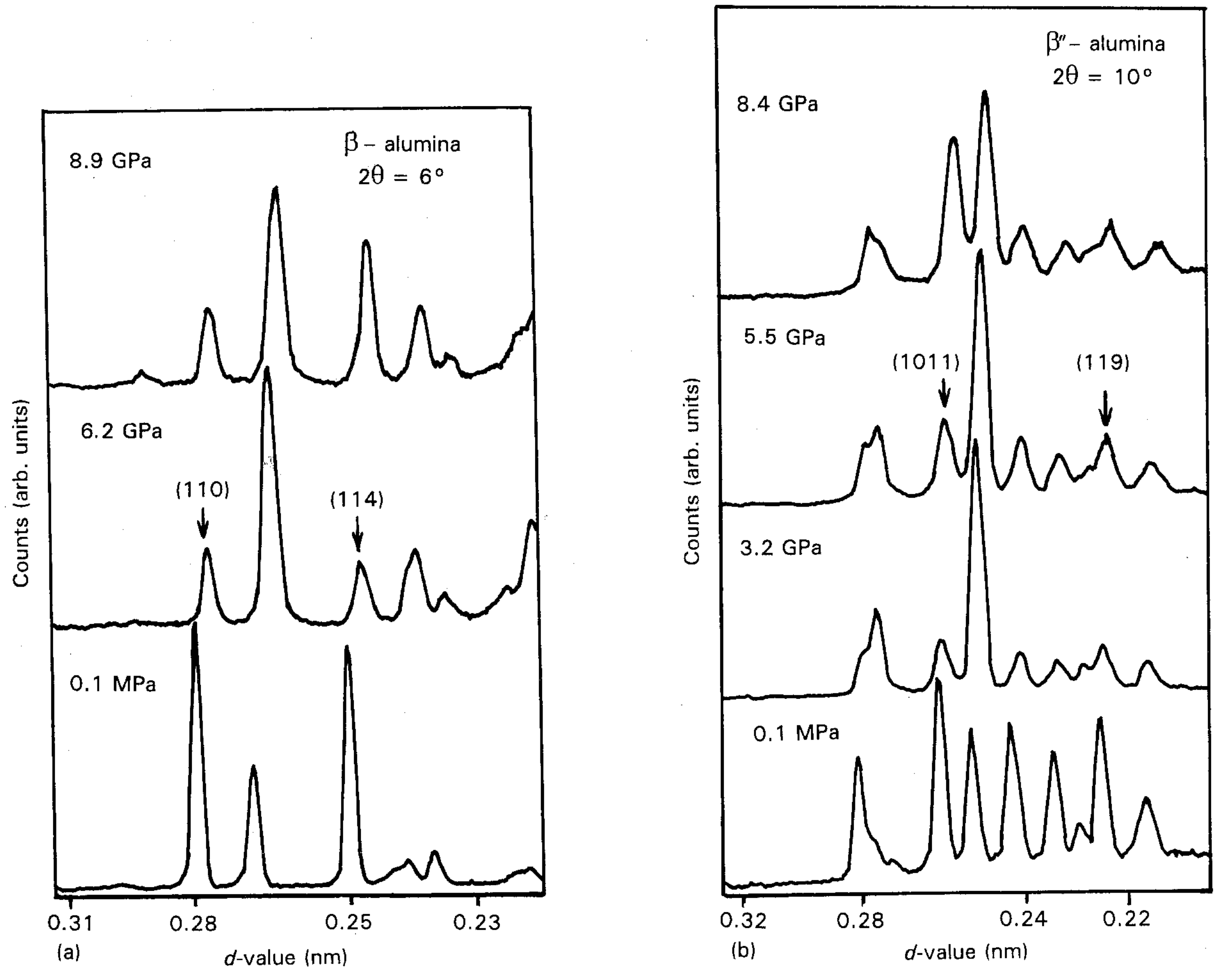

Figure 3 Pressure dependence of X-ray diffraction patterns of (a) β- and (b) β″-aluminas.

TABLE I The comparison between calculated and measured *d* values for β- and β″-aluminas; the lattice constants of the *a*- and *c*-axes were determined by minimizing the sum of square values of difference between calculated and measured *d* values for the following eight diffraction peaks

	JCPDS file 32-1033		Diffraction of β-alumina measured using "MAX80"	
	Observed	Calculated	Observed	Calculated
(1 1 0)	2.797	2.797	2.796	2.795
(1 0 7)	2.681	2.681	2.679	2.678
(1 1 4)	2.505	2.505	2.500	2.503
(2 0 5)	2.134	2.133	2.129	2.132
(2 0 6)	2.036	2.036	2.034	2.034
(2 0 7)	1.935	1.935	1.935	1.934
(2 0 8)	1.836	1.836	1.835	1.835
(2 2 0)	1.399	1.399	1.399	1.397
	$a = 5.594$ Å	$c = 22.53$ Å	$a = 5.589$ Å	$c = 22.51$ Å

	JCPDS file 31-1262		Diffraction of β″-alumina measured using "MAX80"	
	Observed	Calculated	Observed	Calculated
(1 0 11)	2.584	2.548	2.591	2.591
(1 1 6)	2.507	2.508	2.515	2.512
(1 1 7)	2.422	2.422	2.426	2.426
(2 0 4)	2.336	2.334	2.338	2.338
(1 1 9)	2.241	2.242	2.246	2.247
(2 0 7)	2.168	2.168	2.167	2.171
(2 0 10)	1.969	1.968	1.973	1.972
(2 2 0)	1.403	1.403	1.406	1.405
	$a = 5.613$ Å	$c = 33.55$ Å	$a = 5.620$ Å	$c = 33.62$ Å

diffraction pattern is presented in Fig. 3. The diffraction peaks shift to the smaller *d* value side with increasing pressure. The relative intensity markedly changed in the low pressure region, because of the large deformation of the sample assembly at the beginning of pressure loading. Therefore, the crystals contained in the teflon vessel change their orientation with the deformation of the vessel. As the deformation becomes smaller with increasing pressure, the relative intensity change also becomes small in the higher pressure region, as found in Fig. 3.

The lattice constants of the *a*- and *c*-axes at high pressures were determined from eight diffraction peaks by using the method mentioned above. The pressure dependence of the lattice constants of the *a*- and *c*-axes for sodium β- and β″-aluminas is shown in Fig. 4. The lattice constants of the *a*- and *c*-axes of both aluminas linearly decreased with increasing pressure. The relative decrease of the *a*- and *c*-axes is shown in Fig. 5 as a function of pressure. The compression of the *a*-axis is comparable in both sodium aluminas. The compressibilities of sodium β- and β″-alumina along the *a*-axis were $1.5 \pm 0.2 \times 10^{-12}$ and $1.7 \pm 0.2 \times 10^{-12}\ \mathrm{Pa}^{-1}$, respectively. For the *c*-axis, β-alumina is more compressive than β″-alumina. Compressibilities along the *c*-axis of $2.9 \pm 0.2 \times 10^{-12}$ and $1.6 \pm 0.2 \times 10^{-12}\ \mathrm{Pa}^{-1}$ were obtained for sodium β- and β″-aluminas, respectively. The compressibility of the *c*-axis obtained for β-alumina is comparable with the reported value ($2.3 \pm 0.5 \times 10^{-12}\ \mathrm{Pa}^{-1}$) [5].

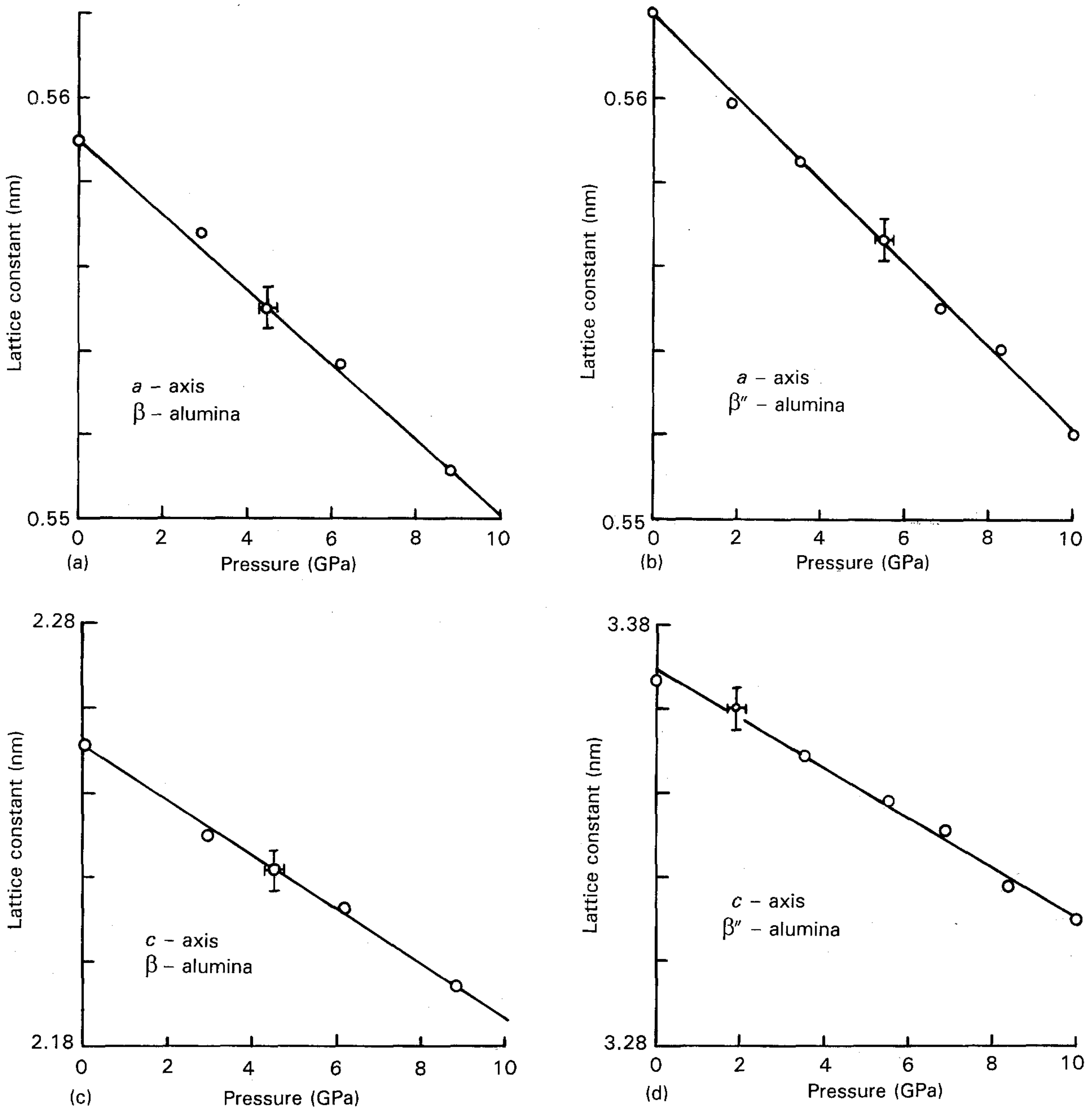

Figure 4 Pressure dependence of the lattice constants of the (a, b) *a*- and (c, d) *c*-axes for β- (a, c) and β''-aluminas (b, d).

The compressibility of α-alumina is also shown by the dotted line in Fig. 5. For the *a*-axis, the compressibilities of β- and β''-aluminas are larger than that of α-alumina. The lattice constant of the *a*-axis is 4.763 Å for α-alumina. As the lattice constant of the *a*-axis of β- and β''-aluminas is larger than that of α-alumina, it is considered that the crystal structure of β- and β''-aluminas is more loose than that of α-alumina and the former gives the larger compressibility. For the *c*-axis, β- and β''-aluminas also show a larger compressibility than that of α-alumina. This is explained by the loosely coupled conduction planes of sodium ions in β- and β''-aluminas. It should be emphasized that the compressibility of β-alumina is larger than that of β''-alumina. This difference can be explained by the different stacking of oxygen layers in these crystals [17]. The arrangement of oxygen and sodium ions in conduction planes of these crystals is schematically shown in Fig. 6. The adjacent spinel-type blocks which contain four layers of cubic close-packed oxygen ions are loosely held through the spacer oxygen atom hatched in Fig. 6. In β''-alumina, the close packing of oxygen atoms is maintained through the crystal. On the other hand, the continuity of the close packing of oxygen atoms is stopped in the conduction plane because of the mirror symmetry in β-alumina. The spacer oxygen ions are tetrahedrally connected with the neighbouring oxygen ions in the spinel-type block above and below the conductive plane in β''-alumina. In β-alumina, the oxygen atom in the conduction plane locates at the center of a triangular prism of six oxygen atoms which are contained in the spinel-type blocks. The density of sodium ions in the conduction plane of β''-alumina is twice as large as that of β-alumina. On the basis of these structural differences in the connection between the spinel-type blocks and the difference in sodium content of the conduction plane, it is concluded that the connection

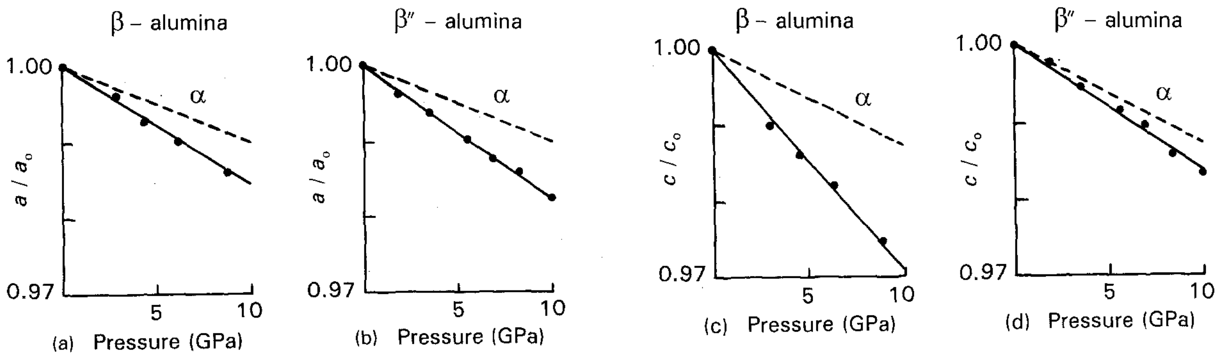

Figure 5 Pressure dependence of the relative compression of the (a, b) *a*- and (c, d) *c*-axes for β- (a, c) and β″-aluminas (b, d).

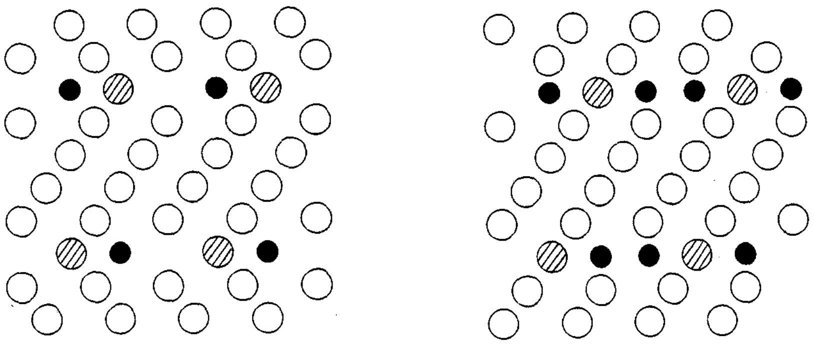

(a) β – alumina (b) β″ – alumina

Figure 6 Crystal structure of (a) β- and (b) β″-aluminas parallel to the *c*-axis. ○: O^{2-} ion in the spinel-type block, ▨: O^{2-} ion in the conduction plane, ●: Na^+ ion. The aluminium ions are not shown.

in β-alumina is looser than in β″-alumina. Therefore, the conduction layer in β-alumina is more compressive than in β″-alumina for compression perpendicular to the layer.

4. Conclusions

The compressibilities of the *a*- and *c*-axes for β- and β″-aluminas were determined up to 10 GPa from the pressure dependence of X-ray diffraction measured at room temperature using synchrotron radiation as an X-ray source. For the *a*-axis, the compressibilities of β- and β″-aluminas are $1.5 \pm 0.2 \times 10^{-12}$ and $1.7 \pm 0.2 \times 10^{-12}$ Pa^{-1}, respectively. These values are larger than that of α-alumina. For the *c*-axis, the compressibilities of β- and β″-aluminas are $2.9 \pm 0.2 \times 10^{-12}$ and $1.6 \pm 0.2 \times 10^{-12}$ Pa^{-1}, respectively. These values are larger than that of α-alumina. These large compressibilities in β- and β″-aluminas are explained by the existence of a loosely coupled conduction plane. Along the *c*-axis, β-alumina has a larger compressibility than that of β″-alumina because of the difference in the stacking of spinel-type blocks. The close packing of oxygen atoms is maintained through the β″-alumina crystal. On the other hand, the continuity of the close packing of oxygen atoms is stopped in the conduction plane because of the mirror symmetry in β-alumina.

Acknowledgement

The authors are grateful to Dr T. Kikegawa of the National Laboratory for High Energy Physics for many valuable discussions concerning the use of the MAX80 high-pressure X-ray diffraction system.

References

1. J. T. KUMMER, in "Progress in solid state chemistry", Vol. 7 edited by H. Reiss and J. O. McCaldin (Pergamon Press, New York, 1972) p. 141.
2. J. H. KENNEDY, in "Solid electrolytes", edited by S. Geller (Springer Verlag, Berlin, 1977) p. 105.
3. C. B. CHOUDHARY, H. S. MAITI and E. C. SUBBARAO, in "Solid electrolytes and their applications", edited by E. C. Subbarao (Plenum Press, New York, 1980) p. 49.
4. G. C. FARRINGTON, B. DUNN and J. O. THOMAS, in "High conductivity solid ionic conductors", edited by T. Takahashi (World Scientific, New Jersey, 1989) p. 327.
5. R. H. RADZILOWSKI and J. T. KUMMER, *J. Electrochem. Soc.* **118** (1971) 714.
6. K. ITOH, K. KONDO, A. SAWAOKA and S. SAITO, *Jpn. J. Appl. Phys.* **14** (1975) 1237.
7. R. H. RADZILOWSKI and J. T. KUMMER, *Rev. Sci. Instrum.* **52** (1971) 727.
8. M. J. GILLAN and M. DIXON, *Solid State Ionics* **5** (1981) 593.
9. J. MOSCINSKI and P. W. M. JACOBS, *Proc. R. Soc. Lond. A* **398** (1985) 173.
10. T. KIKEGAWA, O. SHIMOMURA, H. IWASAKI, S. SATO, A. MIKUNI, A. IIDA and N. KAMIYA, *Rev. Sci. Instrum.* **60** (1989) 1527.
11. O. SHIMOMURA, *Physica B C* **139** (1986) 292.

12. D. L. DECKER, in Proceedings of the 7th International AIRAPT Conference, High Pressure Science and Technology, Lecreusot, July 1979, edited by B. Vodar and Ph. Marteau (Pergamon Press, Oxford, 1980) p. 259.
13. C. R. PETERS, M. BETTMAN, J. L. MOORE and M. D. GLICK, *Acta Crystallogr.* **B27** (1971) 1826.
14. G. YAMAGUCHI and K. SUZUKI, *Bull. Chem. Soc. Jpn* **41** (1968) 93.
15. I. YASUI and T. DOREMUS, *J. Amer. Ceram. Soc.* **60** (1977) 296.
16. L. ZU-XIANG, in "High conductivity solid ionic conductors", edited by T. Takahashi (World Scientific, New Jersey, 1989) p. 223.
17. L. L. HENCH and J. K. WEST, in "Principles of electronic ceramics" (John Wiley & Sons, New York, 1990) p. 161.

Received 8 May 1992
and accepted 5 March 1993